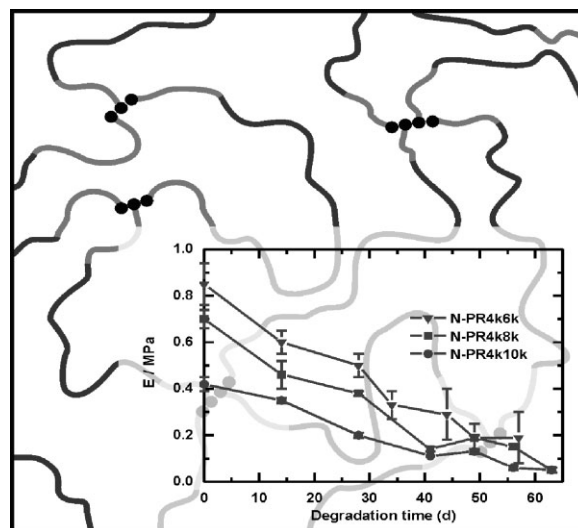


# Hydrolytic Degradation Behavior of Poly(*rac*-lactide)-*block*-poly(propylene glycol)-*block*-poly(*rac*-lactide) Dimethacrylate Derived Networks Designed for Biomedical Applications

Christian Wischke,<sup>a</sup> Giuseppe Tripodo,<sup>a</sup> Nok-Young Choi, Andreas Lendlein\*

For polymer-based degradable implants, mechanical performance and degradation behavior need to be precisely controlled. Based on a rational design, this work comprehensively describes the properties of photo-crosslinked polymer networks prepared from poly(*rac*-lactide)-*block*-poly(propylene glycol)-*block*-poly(*rac*-lactide) dimethacrylate precursors during degradation. By varying the length of poly(*rac*-lactide) blocks connected to a central 4 kDa poly-ether block, microphase separated networks with adjustable crosslinking density, hydrophilicity/hydrophobicity ratio, thermal, and mechanical properties are obtained. The materials are characterized by a low water uptake, controlled mass loss, and slowly decreasing wet-state *E* moduli in the kPa range.



## 1. Introduction

The design of biomedical polymers with tunable properties is required for potential applications in several fields such as in regenerative medicine,<sup>[1–3]</sup> implantable devices,<sup>[4]</sup> prostheses,<sup>[5]</sup> bone and cartilage regeneration,<sup>[6]</sup> or con-

trolled drug release.<sup>[7]</sup> Concerns on the suitability of existing materials to fit future requirements have led to substantial efforts to provide new materials, e.g., also for drug delivery.<sup>[8–11]</sup>

In this context, the degradability of the implanted material is a desired feature and the predominantly employed strategy to enable degradation is the introduction of hydrolytically sensitive bonds in the backbone of synthetic polymers. Degradable polymer segments may be combined with non-degradable, but excretable polymer segments, resulting in partially degradable materials. Polyesters such as from dilactides (PLA),  $\epsilon$ -caprolactone (PCL), or diglycolide (PGA) and their copolymers are among the most intensively studied hydrolytically degradable polymers. The different ester bonds, chemical structures of repeating units, sequence structures, and morphologies are

C. Wischke, G. Tripodo, A. Lendlein  
Center for Biomaterial Development and Berlin-Brandenburg  
Center for Regenerative Therapies, Institute of Polymer Research,  
Helmholtz-Zentrum Geesthacht, Kantstrasse 55, 14513 Teltow,  
Germany  
E-mail: andreas.lendlein@hzg.de  
N.-Y. Choi  
Present address: BASF SE, Engineering Plastics, 67058  
Ludwigshafen, Germany

<sup>a</sup> C. Wischke and G. Tripodo contributed equally to this work.

associated with different degradation rates. Copolymerization often is a suitable method to alter degradation kinetics, e.g., for copolymers from dilactides and diglycolide (PLGA), which show degradation rates depending on the molar ratio of the comonomers. In amorphous PLGA<sup>[12]</sup> as well as in semi-crystalline poly[( $\epsilon$ -caprolactone)-*co*-glycolide],<sup>[13–15]</sup> diades consisting of two glycolide units serve as weak link during the degradation process. Additionally, for semi-crystalline copolymers, the glycolide content effects the materials capability to form crystallites, which are not instantly subject of hydrolysis. While non-crosslinked bulk-degrading (co)polyesters are often associated with a discontinuous decrease in sample weight with a risk for sudden rapid mass loss, improved implant materials should show controllable mass loss and mechanical properties during degradation.

Different approaches were employed to adjust the mechanical and degradation properties of linear polyesters such as brittle PLA. For instance, different alkanes or terpenes were incorporated in PLA films to disturb PLA crystallization and increase its elasticity,<sup>[16]</sup> but this approach can be expected to result only in porous materials and might be associated with issues of biocompatibility due to the residual additives. Blending of brittle PLA with poly(propylene glycol) (PPG) as a 'macromolecular plasticizer' led to a reduced glass transition temperature  $T_g$  and higher elasticity of the material, particularly when using PPG of low molecular weight ( $\bar{M}_n = 425$  Da).<sup>[17]</sup> However, if PPG is only physically incorporated, it will likely be extracted in water, possibly resulting in strong changes in mechanical properties after transfer in a physiological environment. The concept of covalently anchoring polyethers such as poly(ethylene glycol) (PEG) in PLA or PLGA to form linear diblock, triblock, multiblock, star block, and graft copolymers led to a large variety of multiphase materials with relevance for biomedical applications. In these materials, PEG acts as a hydrophilic domain and allows for diffusion controlled protein release as well as a more continuous pattern of mass loss during degradation.<sup>[18,19]</sup> Here, the polyether segment can be regarded as 'non-degradable' compared to the much higher degradation rates of the (co)polyesters.

A general approach to control the materials mechanical properties and the mass loss rates during degradation, is the covalent crosslinking of copolyester networks.<sup>[20]</sup> These networks can be prepared from linear oligo/poly(co)esters with methacrylated end groups by photo-crosslinking (UV irradiation). They can be adjusted in their mechanical and thermal properties and in their degradation pattern by qualitatively varying the methacrylated network precursor or by controlling the crosslinking density (i.e., precursor segment length).<sup>[21–25]</sup> The synthesis and degradation behavior of such polymer networks based on homopolyester or random copolyester segments as well as of two-

phase networks with a major polymethacrylate phase crosslinked by copolyester telechelics (AB networks) were reported.<sup>[26–29]</sup> Importantly, the sequence structure of copolymers can largely affect the hydrolytic degradation of copolyester materials.<sup>[15,30]</sup>

Networks from triblock poly(*rac*-lactide)-*block*-poly(propylene glycol)-*block*-poly(*rac*-lactide) dimethacrylate precursors have been communicated to show shape-memory properties and principal capability for degradation.<sup>[31]</sup> Networks from triarm PPG-PLA triol precursors have been obtained by crosslinking with toluene diisocyanate, but the mechanical or degradation properties under physiological conditions have not been reported.<sup>[32]</sup> Furthermore, linear PLA-PPG-PLA dimethacrylate precursors have been photocopolymerized with 2-hydroxyethylmethacrylate (HEMA) in the presence of a radical initiator to AB networks, which showed a non-linear hydrolytic mass loss<sup>[33]</sup> and compression moduli in the MPa range for both, the networks with and without calcium phosphate loading as potential bone adhesives.<sup>[34]</sup>

The focus of this study is the comprehensive analysis of the properties of multiphase networks from PLA-PPG-PLA precursors during degradation. Importantly, these properties can best be benchmarked in a direct side-by-side comparison with other classes of polymer networks obtained and characterized by comparable synthetic and analytical techniques as reported in here.

## 2. Experimental Section

### 2.1. Materials

Atactic PPG ( $\bar{M}_n = 4000$  Da, Aldrich) was dried under vacuum at 70 °C for at least 3 h. Triethylamine (>99%, Merck) was distilled over CaH<sub>2</sub> ( $\approx 95\%$ , Merck) and stored over molecular sieves (4 Å, Merck). Methacryloyl chloride ( $\geq 97\%$ , Fluka), dibutyltin oxide (DBTO) (purum, Fluka) and *rac*-dilactide (Aldrich, mixture of 93.8 mol% D,D- and L,L-dilactide and 6.2 mol% *meso*-dilactide) were used as received. All solvents (Sigma-Aldrich) were of pro analysis (p.a.) or HPLC quality. Dichloromethane (CH<sub>2</sub>Cl<sub>2</sub>) p.a. was dried over molecular sieves (4 Å). Hexane fraction (Exxon Mobile) was used without further purification.

### 2.2. Methods

#### 2.2.1. Synthesis of Poly(*rac*-lactide)-*block*-poly(propylene glycol)-*block*-poly(*rac*-lactide) Triblock Precursors and Corresponding Networks

The principle of the precursor syntheses was reported before.<sup>[31]</sup> Here, *rac*-dilactide and PPG ( $\bar{M}_n = 4000$  Da) at different weight ratios and 0.3 mol% (PR4k8k-diol: 0.1 mol%) DBTO (referring to *rac*-dilactide) were stirred for 20 h at 130 °C under a nitrogen atmosphere. After purification by precipitation, the macrodiols were dissolved in dry tetrahydrofuran (THF) under a nitrogen atmosphere. Upon cooling in

an ice bath, four equivalents of dry triethylamine (TEA) and methacryloyl chloride were added dropwise and the mixture was stirred for 3 d at room temperature. The precipitated ammonium salt was separated by filtration and unreacted methacryloyl chloride and excess triethylamine were removed by evaporation. The concentrated filtrate was precipitated in a mixture of hexane/diethyl ether/methanol (18/1/1) to remove traces of salt and subsequently reprecipitated from a CH<sub>2</sub>Cl<sub>2</sub> solution in hexane. Networks were synthesized between glass plates with spacers by UV irradiation for 20 min ( $\lambda_{\text{max}}$ : 308 nm; excimer laser, Heraeus Noblelight GmbH, Hanau, Germany) at 70 °C. The obtained films were weighed ( $m_{\text{iso}}$ ), first immersed in diethyl ether overnight, subsequently extracted with chloroform to remove non-crosslinked polymer segments and other impurities (24 h), weighed in the swollen state ( $m_s$ ), and finally dried (vacuum, 50 °C to 70 °C) until a constant weight ( $m_d$ ) is reached. The following terminology was applied: N-PR( $\bar{M}_{n, \text{PPG}}$ )k( $\bar{M}_{n, \text{macrodiol}}$ )k, where “N” stands for “network”, “P” stands for PPG, and “R” stands for poly(*rac*-lactide); e.g., N-PR4k6k is a network derived from triblock macrodiols with a 4 kDa central PPG block and a  $\bar{M}_n$  of 6 kDa. The diols and corresponding dimethacrylates were indicated as PRxyk-diols and -DMA, respectively.

## 2.2.2. Synthesis of Oligo( $\epsilon$ -hydroxycaproate)-*co*-glycolate] Precursors and Corresponding Networks

Macrodiols from  $\epsilon$ -caprolactone and diglycolide were prepared by ring-opening (co)polymerization in the presence of DBTO as catalyst as reported before with subsequent purification.<sup>[14,26]</sup> After reaction of the copolyesterdiols with methacryloyl chloride to dimethacrylates, the N-CG( $\chi_G$ )- $\bar{M}_n$  materials were obtained, where “N” stands for “network” and “CG” for “ $\epsilon$ -caprolactone” and “glycolide”; e.g., N-CG(13)-10 is a network derived from oligo CG precursors with a glycolide molar content  $\chi_G$  of 13 mol% and  $\bar{M}_n = 10$  kDa.<sup>[26]</sup> AB networks abbreviated as AB-CG( $\chi_G$ )- $\bar{M}_n$  were obtained when the copolyester dimethacrylates were photocrosslinked in the presence of 60 wt% *n*-butyl acrylate.<sup>[26]</sup>

## 2.2.3. Polymer Characterization Techniques

DSC studies were performed on a DSC 7 equipped with a TAC 7/DX and CCA 2 (Perkin-Elmer, Waltham, USA) in sealed aluminium pans with heating and cooling rates of 10 K · min<sup>-1</sup>. The glass transitions temperatures ( $T_g$ ) and corresponding changes in heat capacity ( $\Delta C_p$ ) were determined from the data obtained in the second heating run.

Tensile tests were performed on dumbbell-shaped specimens with a gauge length of 3.0 mm and a total length of 10.0 mm on a Zwick 2.5N1S, (Zwick GmbH & Co., Ulm, Germany) equipped with a 50 N load cell. The gauge width and the thickness of the specimen were determined with a slide gauge (precision 0.05 mm) and a micrometer screw (precision 0.005 mm), respectively. The instrument was located in an air-conditioned room at 22 °C and 55% relative humidity, under which conditions freshly prepared materials were characterized in the dry state. Additionally, tensile tests were performed in water at 37 °C after 3 h of equilibration. The deformation rate for all tests was 10 mm min<sup>-1</sup>.

The  $\bar{M}_n$  was determined by means of <sup>1</sup>H-NMR on a Varian Inova 400 MHz spectrometer in CDCl<sub>3</sub> at room temperature, using tetramethylsilane as an internal standard. The degree of methacrylation by <sup>1</sup>H-NMR was calculated by comparing the integral of the two protons of the methacrylic double bond at  $\delta = 6.20$  and 5.63

with that of the three protons of PPG methyl group at  $\delta = 1.09$  and 1.18–1.10. Gel permeation chromatography (GPC) with universal calibration was performed on a mixed D column (600 mm × 7.5 mm, Polymer Laboratories Ltd.) in chloroform with a T60A dual detector (Viscotek GmbH) and an RI detector 8721 (ERC Inc.). Data were evaluated using TriSEC GPC-Viscometry Module Software (Version 3.0, Viscotek GmbH).

## 2.2.4. Hydrolytic Degradation Experiments

The hydrolysis experiments were performed with planar samples (10 × 15 × 0.5 mm<sup>3</sup>) at 37 °C in 15 mL of a pH = 7.0 phosphate buffer (0.1 mol · L<sup>-1</sup> Na<sub>2</sub>HPO<sub>4</sub>, 0.063 mol · L<sup>-1</sup> KH<sub>2</sub>PO<sub>4</sub>; supplemented with 0.25 g · L<sup>-1</sup> NaN<sub>3</sub>), which are sufficient to buffer 0.085 mol of acid.

The water uptake  $H$  of films during the degradation study was determined from the weight ratio of wet and dried (1 mbar, 30 °C) samples at each specific time point. The mass loss  $\mu_{\text{rel}}$  was calculated from the weight ratio of dried samples at a specific time point and the initial sample weight before degradation. The degree of swelling ( $Q$ ) of a polymer network, which is defined as the ratio of the swollen volume at equilibrium to the initial volume, was calculated according to Equation 1:<sup>[35]</sup>

$$Q = 1 + \frac{\rho_2}{\rho_1} \left( \frac{m_s}{m_d} - 1 \right), \quad (1)$$

where  $\rho_1$  and  $\rho_2$  are the densities of the swelling solvent (CHCl<sub>3</sub>) and the polymer network, respectively, while  $m_s$  and  $m_d$  represent the mass of the swollen and of the dried network. Samples from the degradation study were dried first for water removal before swelling in CHCl<sub>3</sub>. The quantity of network components extractable with CHCl<sub>3</sub> was expressed by the gel content  $G$ :

$$G = m_d/m_{\text{iso}}, \quad (2)$$

where  $m_d$  is the mass of dried samples after extraction and  $m_{\text{iso}}$  is the mass of samples as isolated from the degradation study (after drying for water removal).

## 3. Results and Discussion

### 3.1. Network Design Aspects and Rationale for Networks from Triblock Precursors

The degradation pattern of networks prepared from poly(*rac*-lactide)-*block*-poly(propylene glycol)-*block*-poly(*rac*-lactide) triblock precursors was compared to that of other networks containing degradable (co)polyester segments. To allow conclusions on the impact of the type of (co)monomers and molecular architecture on hydrolytic degradation, only materials prepared with the same experimental setup, being derived from linear precursors of similar chain length as analyzed by the same analytical procedures, and crosslinked by methacrylate chemistry should be compared.

A first set of degradable polymer networks (Figure 1A) employed semi-crystalline poly( $\epsilon$ -caprolactone) as homopolymer telechelics [e.g., N-CG(0)-10] in order to avoid rapid



**Figure 1.** Scheme of network structures. (A) Networks from oligo[ $\epsilon$ -caprolactone]-*co*-glycolide] dimethacrylate precursors [N-CG( $\chi_G$ )- $\bar{M}_n$ ], where  $\epsilon$ -caprolactone can crystallize depending on  $\chi_G$ . Modified figure reproduced with permission,<sup>[36]</sup> copyright 2010, Elsevier. (B) Networks from oligo[ $\epsilon$ -caprolactone]-*co*-glycolide] dimethacrylate precursors copolymerized with *n*-butyl acrylate to AB networks [AB-CG( $\chi_G$ )- $\bar{M}_n$ ]. Modified figure reproduced with permission,<sup>[29]</sup> copyright 2010, Wiley-VCH Verlag GmbH & Co. KGaA. (C) Networks from poly(*rac*-lactide)-*block*-poly(propylene glycol)-*block*-poly(*rac*-lactide) triblock precursors with short poly(*rac*-lactide) blocks. The polymer networks contain: (co)oligoester segments (—), which in some cases can crystallize (==), covalent netpoints (●) from photocrosslinking by acrylate chemistry, poly(*n*-butylacrylate) segments (—), and/or PPG segments (—).

water uptake and degradation.<sup>[26]</sup> Since the polyester bonds in poly( $\epsilon$ -caprolactone) are relatively stable in an aqueous environment, diglycolide was copolymerized with  $\epsilon$ -caprolactone to yield materials [e.g., N-CG(13)-10], in which the water uptake is enhanced, crystallinity of poly( $\epsilon$ -caprolactone) is reduced at certain  $\chi_G$ , and hydrolytic degradation is increased due to glycolide serving as weak links.<sup>[26,36]</sup>

As a second set of materials, an additional poly(*n*-butyl acrylate) phase exhibiting a low  $T_g$  was introduced to yield softer AB network materials. These AB networks [e.g., AB-CG(0)-10], in which the degradable (co)polyester segments serve as crosslinkers (Figure 1B), were more hydrophobic and very slowly hydrolytically degrading.

By advancing the concept of multiphase (co)polymer networks and aiming to provide a more hydrophilic material, a third set of networks was proposed, which should be soft and faster degrading than N-CG and AB-CG materials without the use of glycolide units (Figure 1C). These networks base on triblock telechelics, in which PPG segments of intermediate hydrophilicity rather than very hydrophilic PEG are combined with short, degradable polyester segments on both ends. The PLA segments were synthesized from *rac*-dilactide, i.e., a mixture of  $L,L$ - and  $D,D$ -dilactide with a very low *meso*-dilactide content. *Rac*-lactide rather than  $L,L$ -dilactide was used in order to prevent crystallization as expected in the case of isotactic poly(*L*-lactide). A suitable  $\bar{M}_n$  of PPG should be selected in order to establish a microphase separated material with a continuous non-degradable PPG phase and a more hydrophobic, degradable polyester phase.

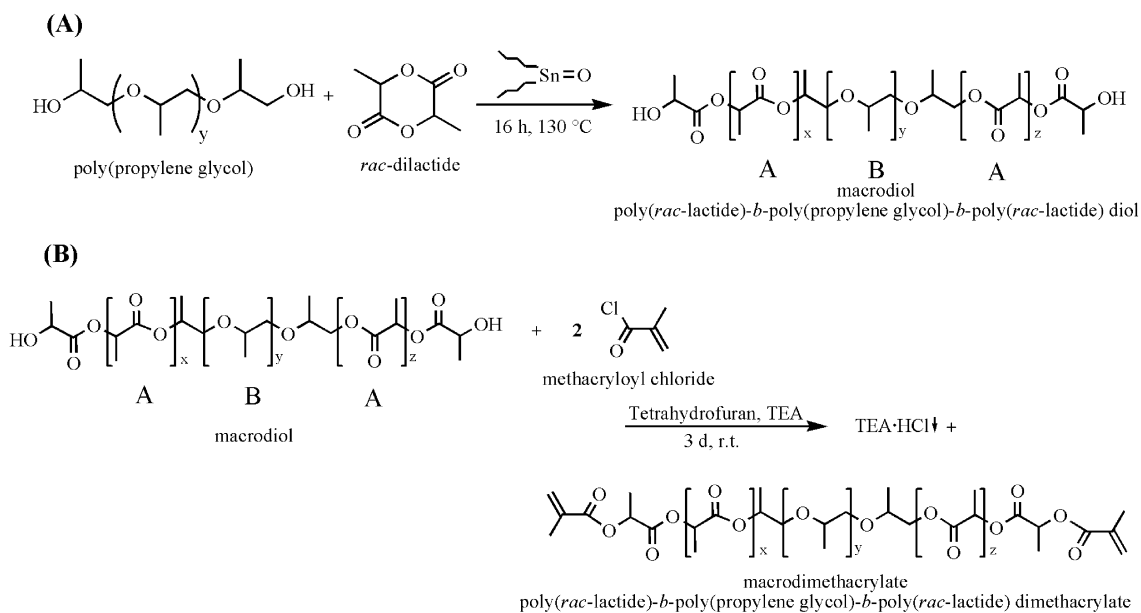
### 3.2. Synthesis and Properties of Triblock Network Precursors

In the literature, it was reported that PPG of very low molecular weight ( $\bar{M}_n = 425$  Da) plasticizes polylactides,<sup>[17]</sup>

which bases on its miscibility with the polyester. Therefore, DSC studies with blends of oligo(*rac*-lactides) and PPG were performed in order to identify a PPG, which would not be miscible with PLA and could be used for a microphase separated material. When PPG of  $\bar{M}_n = 4000$  Da was used, well separated glass transitions of the two homopolymers with no indication of phase mixing were detected. Based on that, PPG of 4000 Da was selected as bifunctional macroinitiator for the ring opening polymerization of *rac*-dilactide in the presence of DBTO as catalyst (Figure 2). In order to control the hydrophilicity/hydrophobicity of the material, the *rac*-dilactide/PPG ratio in the synthesis was increased from 33 to 50 or 60 wt%, respectively. In this way, the average length of the more hydrophobic *rac*-lactide blocks was varied while keeping the  $\bar{M}_n$  of PPG constant.

The obtained macrodiols were purified and characterized by  $^1\text{H-NMR}$ , GPC, and DSC (Table 1). Generally, in a triblock structure, the glass transitions as determined by DSC measurements may correspond to phases associated to different structural elements of the network precursors. The  $T_g$  values in the temperature range of  $-48$  to  $-43$  °C were related to a PPG-rich phase in the polymer matrix. Apparently, in contrast to PPG/PLA blends as tested in DSC screening studies, the covalent binding of the macrodiols to PPG limited phase separation of the macrodiols. Further explanations for shifts in the  $T_g$  might be, e.g., the thermal history of the samples. For PR4k10k-diol, a  $T_g$  of only  $-9$  °C rather than about  $-50$  °C was observed. The very broad thermal transition of this sample (data not shown) indicated a mixed phase of PPG and PLA.

After reaction of macrodiols with methacryloyl chloride (Figure 2),  $^1\text{H-NMR}$  revealed degrees of methacrylation of 56 to 77% and shifts in  $\bar{M}_n$  to higher values (Table 1). The discrepancy for PR4k10k-DMA compared to PR4k10k-diol may be explained by a combination of different effects such as the limited analytical precision of  $^1\text{H-NMR}$  ( $\pm 5\%$ ) and the



challenging purification of these amphiphilic compounds, possibly leading to alteration of the width of the molecular weight distribution and, thus, a shift in  $\bar{M}_n$ . Additionally, after conversion to dimethacrylates, alterations in both the number and temperature of the glass transitions were detected. PR4k10k-DMA now exhibited a  $T_g$  at  $-50^\circ\text{C}$  corresponding to a PPG-rich phase, while the  $T_g$  at  $19^\circ\text{C}$  was related to a PLA-rich mixed phase. For PR4k6k-DMA, spontaneous polymerization was observed during drying, so that the  $T_g$  of the non-crosslinked precursor could not be determined (compare Table 1).

### 3.3. Characterization of the Poly(*rac*-lactide)-*block*-poly(propylene glycol)-*block*-poly(*rac*-lactide) Dimethacrylate-Derived Networks

Upon UV irradiation at  $70^\circ\text{C}$ , terminal methacrylate groups reacted to form netpoints of a covalent network. Depending on the PPG/poly(*rac*-lactide) weight ratio and the precursor chain length, a variation of the properties of the resulting N-PR4k6k, N-PR4k8k, and PR4k10k should be achieved (Table 2). In comparison to a previous study with similar materials,<sup>[31]</sup> slight differences in the precursor synthesis and properties such as the obtained degree of

Table 1. Properties of triblock network precursors (n.a.: not applicable; n.d.: not determined).

Sample	$\bar{M}_n$ [Da]		$\bar{M}_w$ [Da]	PD <sup>a)</sup>	$D_a$ <sup>b)</sup>	$T_g$	$\Delta C_p$
	<sup>1</sup> H-NMR	GPC	GPC	GPC	[%]	[ $^\circ\text{C}$ ]	[ $\text{J} \cdot \text{g}^{-1} \cdot \text{K}^{-1}$ ]
PR4k6k-diol	6 100	6 000	8 200	1.4	n.a.	$-43$	0.39
PR4k6k-DMA	6 400	n.d.	n.d.	n.d.	77	n.d. <sup>c)</sup>	n.d. <sup>c)</sup>
PR4k8k-diol	7 900	7 700	9 700	1.3	n.a.	$-48$	0.58
PR4k8k-DMA	8 000	n.d.	n.d.	n.d.	64	$-41$	0.18
PR4k10k-diol	9 900	6 800	11 300	1.7	n.a.	$-9$	0.26
PR4k10k-DMA	8 500	n.d.	n.d.	n.d.	56	$-50$	0.07
						19	0.07

<sup>a)</sup>Polydispersity; <sup>b)</sup> $D_a$  = degree of methacrylation from <sup>1</sup>H-NMR data; <sup>c)</sup>Sample could not be dried in high vacuum without crosslinking.

**Table 2.** Physical properties of synthesized networks from triblock precursors; mechanical properties were determined with dry materials at room temperature.

Sample	$Q$ [v/v]	$G$ [%]	$\rho_{\text{network}}$ [g · cm <sup>-3</sup> ]	$T_g$ [°C]	$\Delta C_p$ [J · g <sup>-1</sup> · K <sup>-1</sup> ]	$E$ [MPa]	$\sigma_B$ [MPa]	$\epsilon_B$ [%]
N-PR4k6k	5.4	89	1.14	-51 +7	0.29 0.046	1.2 ± 0.01	1.4 ± 0.2	130 ± 10
N-PR4k8k	8.2	64	1.12	-46	0.087	1.4 ± 0.01	2.2 ± 0.6	220 ± 20
N-PR4k10k	10.3	63	1.15	-50 +15	0.042 0.129	4.2 ± 0.3	5.4 ± 0.2	330 ± 10

methacrylation resulted in some alterations of the network properties.

The extent of successful crosslinking of the precursors is measured as gel content  $G$  (non-extractable polymer in the network). With increasing  $\bar{M}_n$  and PLA content, the fixation of the precursors was, however, less efficient. The degree of swelling  $Q$  in CHCl<sub>3</sub> increased with increasing precursor chain length as expected. Interestingly, the  $Q$  values for N-CG<sup>[26]</sup> and N-PR networks were in the same range for similar precursor chain lengths. In addition to the average segment length between the netpoints,  $Q$  is also affected by other parameters such as the polymer/solvent interaction. Still, similar  $Q$  values might indicate similar crosslinking densities. Based on that, different bulk properties of the N-CG and N-PR networks (e.g., mechanical properties) can be related to the precursor's chemical composition, average molecular weight, and sequence structure.

Along with the increase in N-PR precursor chain length, i.e., decrease of the crosslinking density, networks showed increasing dry-state elongation at break ( $\epsilon_B$ ) at room temperature. Additionally, dry-state Young's modulus ( $E$ ) at room temperature increased due to the contribution of glassy domains formed by oligo(*rac*-lactide) segments.

The obtained networks were completely amorphous. Generally, in polymer networks, the influence of free chain ends on  $T_g$  as observed for telechelics is eliminated, because the chain ends are now fixed in the covalent netpoints. In consequence, by exclusion of effects of free chain ends, the impact of the precursor's  $\bar{M}_n$  and composition on phase separation and  $T_g$  can be discussed. In the N-PR networks, a PPG-rich phase and a PLA-rich phase were detected, as previously also evidenced by DMTA studies.<sup>[31]</sup> Apparently, increasing precursor chain lengths did not strongly affect the  $T_g$  of the PPG-rich phase of the network at about -50 °C (Table 2), because the PPG  $\bar{M}_n$  was kept constant. Decreasing  $\Delta C_p$  for the PPG phase with increasing  $\bar{M}_n$  of the precursor may be due to the decreasing PPG content and contributions to the mixed PLA-rich phase. Particularly at high weight content of PPG such as in N-PR4k6k, it can be expected that PPG formed the continuous, rather soft phase, in which individual PLA-rich domains were dispersed. These PLA-rich

domains were formed by short oligo(*rac*-lactide) chains connected to methacrylate netpoints. The  $T_g$  of the PLA-rich phase strongly depended on the precursor composition, i.e., increasing PLA block lengths resulted in increasing  $T_g$  (as one would expect from the Fox equation) and increasing  $\Delta C_p$ . It should be noted that the PLA-rich phase was characterized by a broad glass transition also including the temperature range, in which the  $T_g$  of pure PLA can be expected.

### 3.4. Degradation Behavior of Crosslinked Polymer Networks

To further explore the effect of precursor and network properties on the degradation pattern of N-PR materials, samples were incubated in phosphate buffer at 37 °C and analyzed at various time points. For N-PR4k6k, the experiment had to be stopped earlier due to massive degradation and difficulties to recover the samples.

The mass loss of degraded samples is based on the removal of water soluble degradation products that are no longer covalently bound to the matrix. Mass loss of the triblock precursor-derived materials had no distinct induction period (Figure 3A). By trend, N-PR4k6k (highest PPG content) showed the fastest degradation with 50 wt% mass loss in 130 d. At this time point, differences in mass loss between N-PR4k6k and N-PR4k10k were as large as 30 wt%. These findings reflect the effect of the precursors properties such as the PPG-derived hydrophilicity of the network. For comparison, the mass loss due to hydrolytic degradation of more hydrophobic N-CG and AB-CG is given in Figure 3B. For these networks, degradation in some cases resulted in a rather non-linear mass loss after a long induction period and was generally very slow. In contrast, the triblock precursor-derived networks degraded faster with a continuous mass loss. This, in principle, is in good agreement with data of non-crosslinked PLGA-PEG-PLGA compared to non-crosslinked PLGA.<sup>[19]</sup>

The continuous PPG-rich phase of intermediate hydrophilicity was expected to rule the uptake of water, which is required for polyester hydrolysis (Figure 4). Therefore,



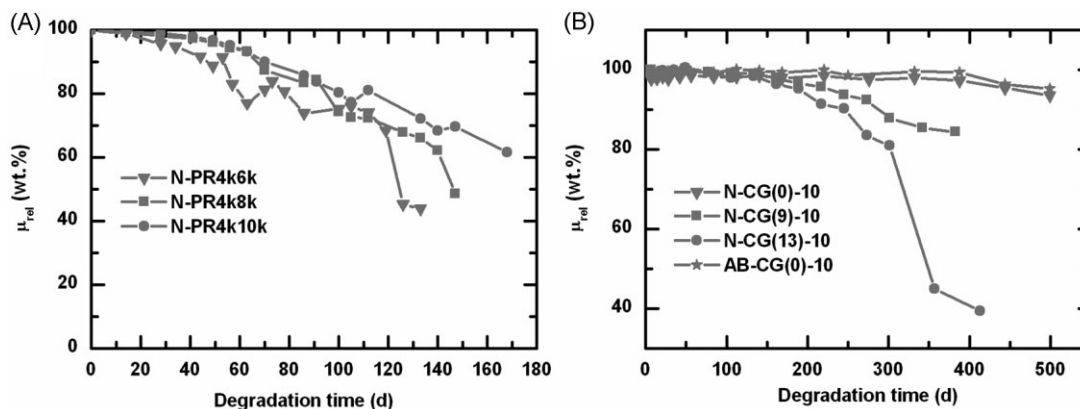


Figure 3. Sample mass loss during their degradation in phosphate buffer at 37 °C. (A) Data of poly(*rac*-lactide)-*block*-poly(propylene glycol)-*block*-poly(*rac*-lactide) triblock precursor-derived networks. (B) Comparison to previously reported networks containing degradable (co)polyester segments. Reproduced with permission,<sup>[26]</sup> copyright 2007, American Chemical Society.

higher PPG contents should allow a faster diffusion of more water into the network, potentially resulting in a faster degradation. However, no clear differences in the initial water uptake could be observed, which occurred rapidly and was surprisingly low at about 1 wt% only. This suggests that extensive initial water uptake was anticipated by the crosslinked network structure. Establishing materials with such low water uptake and thus volume changes despite the large quantity of incorporated hydrophilic segments is a remarkable finding. This will be advantageous for biomedical implants, which should typically not experience major swelling after implantation.

During subsequent degradation, the network with the highest PPG content and lowest precursor molecular weight, i.e., highest crosslinking density, N-PR4k6k, showed lowest water uptake. With increasing precursor molecular weight, water uptake was higher at least after 55 d of degradation. In contrast to mass loss experiments with an almost constant profile, water uptake appeared to have two

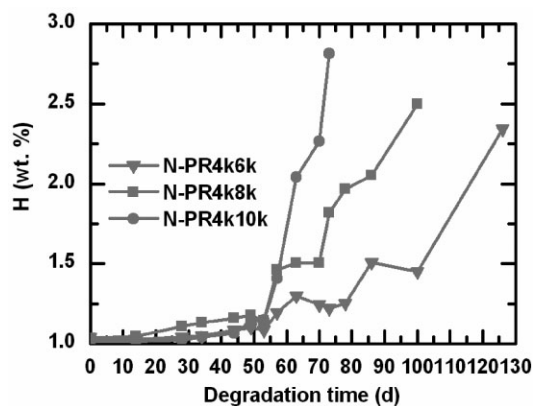


Figure 4. Water uptake of samples during their degradation in phosphate buffer at 37 °C.

phases. It can be assumed that, after a critical extent of chain scissions, the remaining netpoints cannot fully resist the osmotic pressure of the PPG domains and more water is taken up. Importantly, compared to previously reported AB networks from PLA-PPG-PLA dimethacrylate precursors with massive water uptake of 10 to 60 wt% after 14 weeks,<sup>[33]</sup> the materials reported in here have a low water uptake, e.g., only 1.5 wt% for N-PR4k6k after 14 weeks. An explanation for that may be differences in the network architecture and morphology and the presences of numerous pendant OH groups from HEMA in this AB network.<sup>[33]</sup>

However, it has to be stressed that mass loss-based degradation kinetics are not necessarily correlating with the quantity of water uptake, but with i) the access of water to hydrolytically sensitive bonds and ii) the aqueous solubility of degradation products. For shorter oligo(*rac*-lactide) chains, the PLA-rich domains around the methacrylate netpoints may be smaller with a larger surface area-to-volume ratio. Additionally, the  $T_g$  of the PLA-rich phase will be decreased, thus allowing for higher chain mobility and water diffusion rates. In consequence, the shorter polyester segments hydrolyze faster to water soluble products. Furthermore, their removal from the matrix may be more effective for materials from precursors with shorter oligo(*rac*-lactide) blocks.

The capability of N-PR4k6k samples to show a faster mass loss compared to the other N-PR materials while requiring low water uptake for hydrolysis may be advantageous for different reasons. Generally, the available quantity of water might be different at different implantation sites. Therefore, water-induced hydrolytic in vivo degradation of materials with a low maximum water uptake may be less differing when changing implantation sites. Additionally, as mentioned before, strong water uptake and volume increase could result in disadvantageous pressure on adjacent tissue. However, it also has to be noted that a

certain water uptake, e.g., 3 wt% of an initially dense matrix during degradation does not necessarily mean volume changes of the implant, particularly if a mass loss of 30 wt% or more has already resulted in a meso- or macroporous structure.

While mass loss is a measure of network degradation to water soluble products,  $G$  as determined in chloroform is inversely proportional to the quantity of those degradation products, which are no longer crosslinked in the network structure but are not yet water soluble. Therefore,  $G$  is more useful to describe changes in the crosslinked network structure at earlier time points than mass loss.  $G$  decreased most rapidly for N-PR4k6k during first month of degradation as expected (Figure 5A). However, at later time points,  $G$  followed the order N-PR4k10k < N-PR4k8k < N-PR4k6k. This means that the crosslinked network structure is destroyed faster for materials derived from the precursors with higher  $\bar{M}_n$  and PLA content, which contrasts the mass loss data (Figure 3A). Furthermore, this suggests differences in the effect of chain scissions on mass loss and  $G$  for the different N-PR materials. Polyester hydrolysis in materials with short PLA segments apparently resulted in a major quantity of water-soluble products, which diffuse out of the matrix (higher  $\mu_{rel}$ ) and therefore are not detected during chloroform extraction (lower  $G$ ) particularly after 60 d of degradation (Figure 3A and 5A). For N-PR4k8k and N-PR4k10k with longer PLA chain lengths, the opposite appears to be the case, because statistically longer soluble oligo(*rac*-lactide) segments remain attached to PPG 4000 kDa, thus impeding the fragment's solubility in water or causing entrapment by entanglements. Compared to the N-CG and AB-CG networks, degradation as measured by  $G$  and mass loss is faster for the triblock precursor-derived networks (Figure 5B).<sup>[36]</sup>

For comparison of thermal properties, it should be noted that the N-PR materials are fully amorphous and have one or two glass transitions, while N-CG and AB-CG are semi-

crystalline and show a more or less pronounced melting transition as highest thermal transition. However, above their highest thermal transitions  $T_{trans}$  corresponding to either  $T_g$  or  $T_m$  (Figure 6), all materials are in the viscoelastic state. For N-CG and AB-CG materials, degradation-induced slight increases of  $T_{trans}$  correspond to an improved capability of shorter chain to spatially arrange for crystallization. In selected cases [compare N-CG(9)-10, Figure 6B], this could result in changes of the physical state by crystallization at 37 °C. For N-PR materials, no increase in  $T_{trans}$  or crystallite formation were observed, which is a big advantage for a possible application as degradable implant material since crystalline particles may delay degradation.

In order to follow the mechanical properties of these networks during degradation under conditions relevant for a biomedical application, tensile tests were performed in an aqueous environment at 37 °C. In general, due to the increased temperature and the aqueous environment, lower initial  $E$  values were observed for wet samples (Figure 7A) compared to the dry materials at room temperature (Table 2). Interestingly, also the order of the initial  $E$  moduli changed to N-PR4k6k > N-PR4k8k > N-PR4k10k. A possible explanation might be that in water at 37 °C all network phases including the PLA segments were in their viscoelastic state. In consequence, single PLA-rich domains might no longer have strengthened the network as discussed above for dry-state materials at room temperature. Accordingly, the tensile properties were a function of the crosslinking density, which was highest for the material with the highest wet stage  $E$  modulus at 37 °C (N-PR4k6k). During degradation, the  $E$  modulus slowly decreased as aimed for in this study, illustrating the success of the applied concept to design chemically crosslinked polymer networks.

The  $\epsilon_B$  values in the wet state at 37 °C were highest for the material with the lowest crosslinking density (Figure 7C). It has been reported before as an advantageous feature of

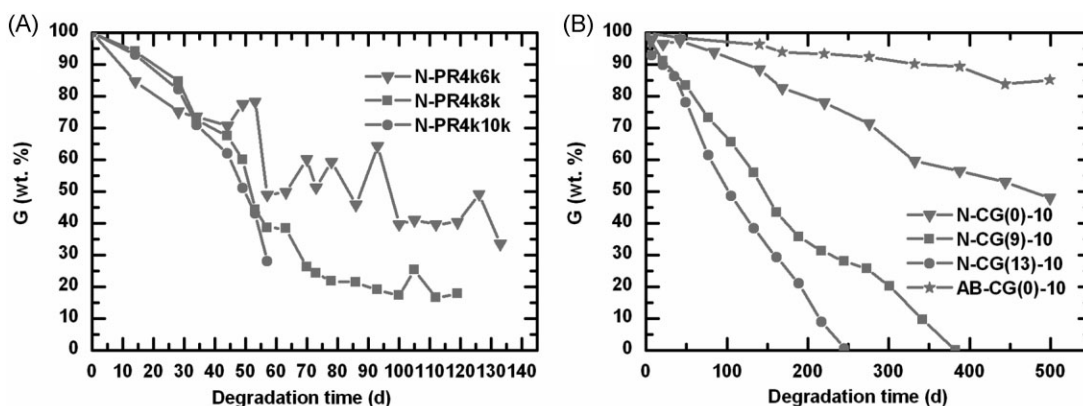


Figure 5. Gel content  $G$  of networks during their degradation in phosphate buffer at 37 °C. (A) Data of poly(*rac*-lactide)-block-poly(propylene glycol)-block-poly(*rac*-lactide) triblock precursor-derived networks. (B) Comparison to other networks containing degradable (co)polyester segments. Selected data were previously reported and are reproduced with permission,<sup>[26]</sup> copyright 2007, American Chemical Society.



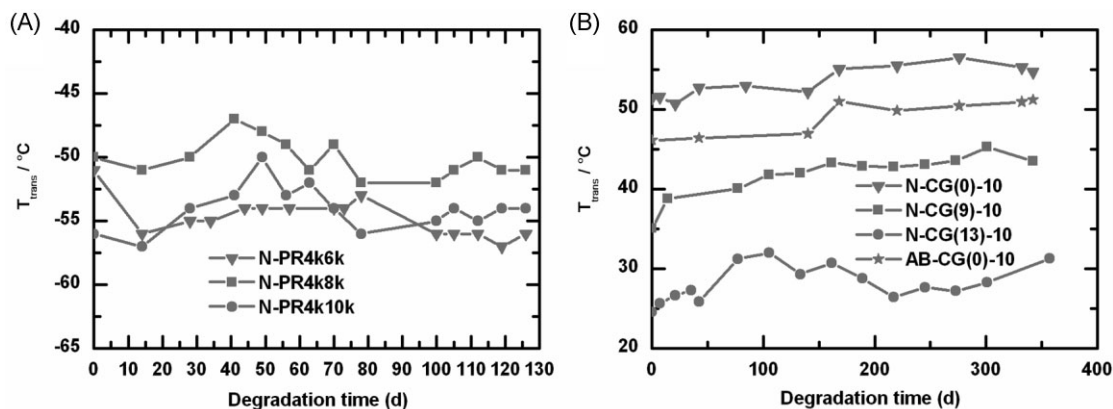


Figure 6. Highest thermal transition of networks during degradation in phosphate buffer at 37 °C as given by the corresponding thermal transition temperature  $T_{trans}$ . (A) Data of poly(*rac*-lactide)-*block*-poly(propylene glycol)-*block*-poly(*rac*-lactide) triblock precursor-derived networks showing a glass transition. (B) Comparison to other networks containing degradable (co)polyester segments showing a melting transition. Selected data were previously reported and are reproduced with permission;<sup>[26]</sup> copyright 2007, American Chemical Society.

crosslinked networks, that elasticity typically increases during degradation in a slow, controlled manner.<sup>[20]</sup> However, here, all materials remained soft and experienced only minor changes in  $\epsilon_B$ . Possibly, increased  $\epsilon_B$  may have been associated with later stages of degradation of N-PR materials when they were too soft to be handled in tensile tests. The comparison with N-CG and AB-CG networks

(Figure 7B, D) illustrates that the N-PR materials were much softer and could be finely tuned in their mechanical properties in the desired kPa range by changes in the block length of the triblock precursors.

Such mechanical properties may be interesting for implants, which are mechanically compatible with soft tissues. In combination with an absence of brittleness

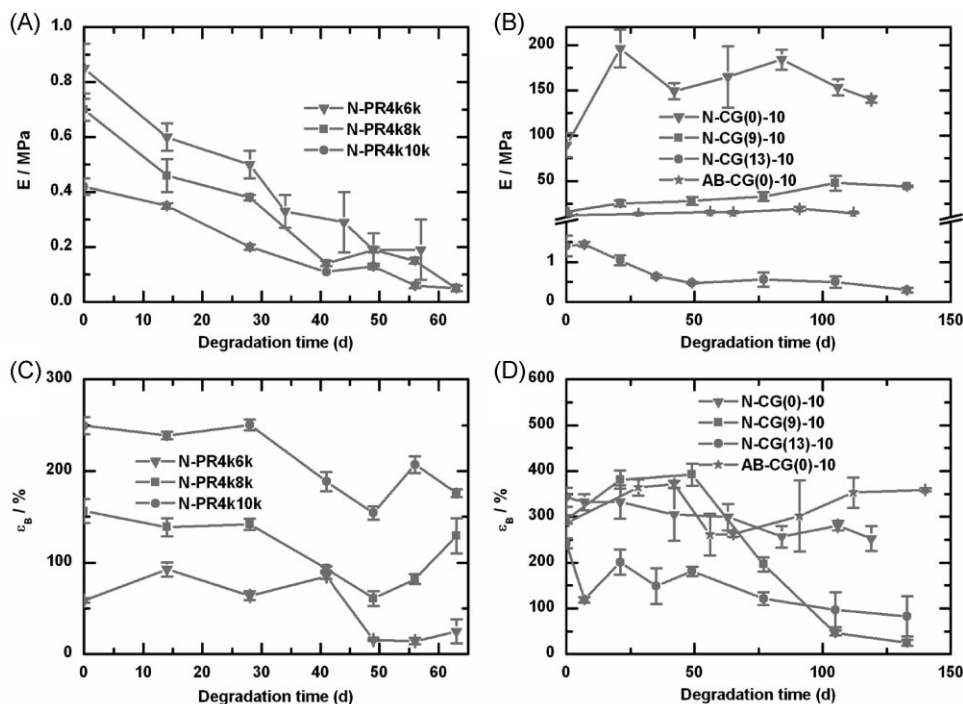


Figure 7. Wet-state mechanical properties of networks as measured at 37 °C during their degradation in phosphate buffer at 37 °C. Data of poly(*rac*-lactide)-*block*-poly(propylene glycol)-*block*-poly(*rac*-lactide) triblock precursor-derived networks including the Young's modulus  $E$  (A) and elongation at break  $\epsilon_B$  (C). For comparison,  $E$  (B) and  $\epsilon_B$  (D) are shown for other networks containing degradable (co)polyester segments. Selected data were previously reported and are reproduced with permission;<sup>[26]</sup> copyright 2007, American Chemical Society.

during degradation, such N-PR materials may be useful as flexible implants for implantation sites that are frequently subjected to deformation or bending such as the abdomen or in the proximity of joints. For example, films might be explored to prevent post-surgical adhesions, possibly in combination with a sustained release of drugs being embedded in the matrix. Finally, it should be noted that the degradation products will be suitable for renal excretion (PPG, D-lactide) or metabolism in the citric acid cycle (L-lactide).

#### 4. Conclusion

This study focused on the degradation behavior of poly(*rac*-lactide)-*block*-poly(propylene glycol)-*block*-poly(*rac*-lactide) dimethacrylate derived networks, which is of high relevance for the performance of these materials in biomedical applications. A profound knowledge is provided suggesting advantageous properties of these networks when aiming for a soft material, which degrades in 6 to 12 months without abrupt changes of its mechanical properties. In particular, the triblock structure with PPG as central block of intermediate hydrophilicity along with the segment length of attached, hydrophobic poly(*rac*-lactide) allows for a control of i) water uptake, ii) the solubility of degradation products, iii) the rate of network breakdown as well as iv) smooth kinetics of mass loss and decrease of *E* modulus without a trend to brittleness. Such soft materials with wet-state *E* moduli in the kPa range may be of high interest for drug releasing implants matching the mechanical properties of the surrounding tissue, as transdermal therapeutic systems, or as membranes to prevent post-surgical adhesion.

**Acknowledgements:** The authors thank the Bundesministerium für Bildung und Forschung (BMBF) for financial support through BioFuture Award 0311867 and Melanie Bonnekessel for support in some experiments.

Received: June 7, 2011; Published online: October 19, 2011; DOI: 10.1002/mabi.201100226

**Keywords:** biomaterials; hydrolytic degradation; polymer networks; poly(propylene glycol); poly(*rac*-lactide)

[1] K. Y. Lee, L. Jeong, Y. O. Kang, S. J. Lee, W. H. Park, *Adv. Drug Delivery Rev.* **2009**, *61*, 1020.

- [2] M. E. Furth, A. Atala, M. E. Van Dyke, *Biomaterials* **2007**, *28*, 5068.
- [3] V. P. Shastri, A. Lendlein, *Adv. Mater.* **2009**, *21*, 3231.
- [4] S. L. Fialho, F. Behar-Cohen, A. Silva-Cunha, *Eur. J. Pharm. Biopharm.* **2008**, *68*, 637.
- [5] J. O. Winter, M. Gokhale, R. J. Jensen, S. F. Cogan, J. F. Rizzo, *Mater. Sci. Eng. C, Biomimet. Supramol. Syst.* **2008**, *28*, 448.
- [6] D. Puppi, F. Chiellini, A. M. Piras, E. Chiellini, *Prog. Polym. Sci.* **2010**, *35*, 403.
- [7] C. Wischke, S. P. Schwendeman, *Int. J. Pharm.* **2008**, *364*, 298.
- [8] A. T. Neffe, B. D. Hanh, S. Steuer, A. Lendlein, *Adv. Mater.* **2009**, *21*, 3394.
- [9] G. Tripodo, G. Pitarresi, G. Cavallaro, F. S. Palumbo, G. Giammona, *Macromol. Biosci.* **2009**, *9*, 393.
- [10] V. Mourino, A. R. Boccaccini, *J. Roy. Soc. Interface* **2010**, *7*, 209.
- [11] H. D. Tang, C. J. Murphy, B. Zhang, Y. Q. Shen, E. A. Van Kirk, W. J. Murdoch, M. Radosz, *Biomaterials* **2010**, *31*, 7139.
- [12] D. Hofmann, M. Entrialgo-Castano, K. Kratz, A. Lendlein, *Adv. Mater.* **2009**, *21*, 3237.
- [13] A. Lendlein, P. Neuenschwander, U. W. Suter, *Macromol. Chem. Phys.* **1998**, *199*, 2785.
- [14] A. Lendlein, P. Neuenschwander, U. W. Suter, *Macromol. Chem. Phys.* **2000**, *201*, 1067.
- [15] A. Lendlein, M. Colussi, P. Neuenschwander, U. W. Suter, *Macromol. Chem. Phys.* **2001**, *202*, 2702.
- [16] H. Sawalha, K. Schroen, R. Boom, *Polym. Eng. Sci.* **2010**, *50*, 513.
- [17] Z. Kulinski, E. Piorkowska, K. Gadzinowska, M. Stasiak, *Biomacromolecules* **2006**, *7*, 2128.
- [18] Y. X. Li, T. Kissel, *J. Controlled Release* **1993**, *27*, 247.
- [19] T. Kissel, Y. X. Li, F. Unger, *Adv. Drug Delivery Rev.* **2002**, *54*, 99.
- [20] A. T. Neffe, G. Tronci, A. Alteheld, A. Lendlein, *Macromol. Chem. Phys.* **2010**, *211*, 182.
- [21] N. Y. Choi, A. Lendlein, *Soft Matter* **2007**, *3*, 901.
- [22] S. Kelch, N. Y. Choi, Z. G. Wang, A. Lendlein, *Adv. Eng. Mater.* **2008**, *10*, 494.
- [23] M. Bertmer, A. Buda, I. Blumenkamp-Hofges, S. Kelch, A. Lendlein, *Biomacromolecules* **2005**, *38*, 3793.
- [24] A. Lendlein, A. M. Schmidt, R. Langer, *Proc. Natl. Acad. Sci. USA* **2001**, *98*, 842.
- [25] J. Zotzmann, A. Alteheld, M. Behl, A. Lendlein, *J. Mater. Sci., Mater. Med.* **2009**, *20*, 1815.
- [26] S. Kelch, S. Steuer, A. M. Schmidt, A. Lendlein, *Biomacromolecules* **2007**, *8*, 1018.
- [27] A. Alteheld, Y. K. Feng, S. Kelch, A. Lendlein, *Angew. Chem. Int. Ed.* **2005**, *44*, 1188.
- [28] A. Lendlein, J. Zotzmann, Y. K. Feng, A. Alteheld, S. Kelch, *Biomacromolecules* **2009**, *10*, 975.
- [29] C. Wischke, A. T. Neffe, S. Steuer, E. Engelhardt, A. Lendlein, *Macromol. Biosci.* **2010**, *10*, 1063.
- [30] M. Vert, S. M. Li, H. Garreau, *J. Biomater. Sci., Polym. Ed.* **1994**, *6*, 639.
- [31] N. Y. Choi, S. Kelch, A. Lendlein, *Adv. Eng. Mater.* **2006**, *8*, 439.
- [32] D. M. Yang, Q. Lu, Z. Y. Fan, S. M. Li, J. J. Tu, W. Wang, *J. Appl. Polym. Sci.* **2010**, *118*, 2304.
- [33] S. M. Ho, A. M. Young, *Eur. Polym. J.* **2006**, *42*, 1775.
- [34] E. A. Abou Neel, G. Palmer, J. C. Knowles, V. Salih, A. M. Young, *Acta Biomater.* **2010**, *6*, 2695.
- [35] G. Malucelli, G. Gozzelino, R. Bongiovanni, A. Priola, *Polymer* **1996**, *37*, 2565.
- [36] C. Wischke, A. T. Neffe, S. Steuer, A. Lendlein, *Eur. J. Pharm. Sci.* **2010**, *41*, 136.